Polymer Chemistry

ROYAL SOCIETY OF CHEMISTRY

PAPER

View Article Online
View Journal | View Issue

Cite this: *Polym. Chem.*, 2025, **16**, 2933

5-Ethylidene-2-norbornene (ENB) and 5-vinyl-2-norbornene (VNB) based alicyclic polyols for the synthesis of polyesters†

Brigita Bratić,[a] Peter Altenbuchner,[b] Thomas Heuser[b] and Bernhard Rieger *[a]

Received 10th March 2025,
Accepted 18th May 2025

DOI: 10.1039/d5py00247h

rsc.li/polymers

Amorphous polyesters derived from rigid alicyclic monomers with high glass transition temperatures are of great interest as potential substitutes for poly(carbonate)s. Therefore, 5-ethylidene-2-norbornene (ENB) and 5-vinyl-2-norbornene (VNB) were identified as interesting diol monomer precursors to enhance the thermal properties of polyesters. The regioselective synthesis of the corresponding diols from ENB and VNB was optimized and the first scale-up experiments gave promising results for a potential large-scale production of these polyester monomers. Moreover, for proof of concept, an alternative procedure was established to synthesize exclusively *branched* diols. Polymerization experiments were conducted with dimethyl terephthalate (DMT) as a model compound to compare the polyesters with commonly used poly(ethylene terephthalate)s. Therefore, a series of polyesters containing *branched* or *linear* regioisomers or a mixture of both regioisomers were produced, and structure–property relationships were investigated using GPC, TGA and DSC analyses. The T_g values ranged from 75 to 103 °C, depending on the *branched* and *linear* moieties in the polyester microstructure and their molecular weights. Moreover, isosorbide (IS) was introduced as a biobased comonomer, resulting in amorphous copolyesters with promising T_gs ranging from 81 to 97 °C.

Introduction

Polymers, with their versatile properties, have become indispensable in today's world since they fulfil a wide range of needs across industries, driving innovation and sustainability efforts. Their adaptability ensures that they will remain at the forefront of technological advancements for years to come.[1,2] The development of new polymer materials is therefore of utmost importance due to the increasing requirements regarding performance and safety.[1–4] One example of increasing safety standards is the impending worldwide ban of bisphenol-A-based polycarbonates (BPA-PC) due to their endocrine disrupting effects and toxicity.[5–8] A potential candidate for the replacement of such widely used BPA-based polymers could be amorphous polyesters, ensuring that they exhibit comparable properties such as high heat resistance and clarity to fulfil market requirements. However, in this regard, most amorphous polyesters are often limited due to their low glass transition temperature (T_g), which is an important thermomechanical property for their practical application in industries such as food packaging materials and coil coatings.[4,9,10] Amorphous polyesters with high T_gs are thermally stable, enabling them to endure higher temperatures without deformation or structure loss. This stability is required in food packaging, where products may undergo heating during processing or storage, as high T_g ensures the shape and barrier properties of packaging materials.[10,11]

Moreover, high T_g polyesters exhibit superior barrier properties against gases, moisture and scents, crucial for preserving product freshness and quality.[12] Additionally, their enhanced mechanical properties ensure better protection for packaged products during handling, transportation and storage.[3] In applications such as coil coating, where the coating must withstand mechanical stresses and deformation, a high T_g guarantees the maintenance of structural integrity.[13]

An option to improve the thermal properties of polyesters is the incorporation of rigid cyclic structures into the polyester backbone, which has already been demonstrated in the literature. For example, tricyclodecanedimethanol (TCD-DM) was studied by the group of Fenouillot resulting in amorphous polyester materials with T_gs ranging from 116 to 163 °C.[14] Among TCD-DM, isosorbide (IS) was studied extensively in the synthesis and modification

[a]*Technical University of Munich, WACKER Chair of Macromolecular Chemistry, Department of Chemistry, D-85748 Garching bei München, Germany. E-mail: rieger@tum.de; Tel: +49 (0)89 289 54448*
[b]*Evonik Operations GmbH, Paul-Baumann-Straße 1, D-45772 Marl, Germany. E-mail: peter.altenbuchner@evonik.com, thomas.heuser@evonik.com*

†Electronic supplementary information (ESI) available: Experimental (monomer synthesis and polymerisation); additional ^{1}H, ^{13}C and DOSY NMR spectra, thermal analysis (TGA and DSC), and GPC data. See DOI: https://doi.org/10.1039/d5py00247h

of polyester materials with varying isosorbide content.[10,14–24] Further interesting examples are 2,2,4,4-tetramethyl-1,3-cyclobutanediol (TMCD),[12,25–27] which is known for the production of high-performance Tritan™ (Eastman), and spiroglycol (SPG),[1] which is used for the production of Akestra™ (Perstorp AB). The substitution of terephthalic acid (TPA) or dimethyl terephthalate (DMT) has been a topic of research in food packaging as well, leading to many examples of dimethyl ester 2,5-furanedicarboxylate (DMFD)-based polyesters with remarkable thermal and barrier material properties.[10,11,28–30] All these polymers exhibit high T_gs and can even be produced from biobased sources.

Nature provides a rich diversity of diene structures, which are potential precursors for the synthesis of diols, yet their availability for large-scale polymer production is often constrained by factors such as reactivity issues, extraction and high cost.[31] With our search for new polyesters in mind, we identified 5-ethylidene-2-norbornene (ENB, **1**) and 5-vinyl-2-norbornene (VNB, **2**) as interesting monomer precursors, a readily available feedstock from the ethylene-propylene-diene monomer (EPDM) industry, which are produced on a multi-million metric ton per year scale.[32] Their bicyclic core not only provides rigidity, but the corresponding diols (**4**) are also accessible *via* a hydroformylation–reduction sequence (Scheme 1). Our research aims to develop an efficient process that offers a new pathway to produce cycloaliphatic diols in a cost-effective and scalable manner. Moreover, this development could enable the production of additional downstream products, such as amines, carboxylic acids, and methyl methacrylates. Furthermore, the nature of the *exo*cyclic double bonds in ENB (**1**) and VNB (**2**) allows control of the regioselectivity (*linear vs. branched* diols). Thus, the polyester backbone can be modified, and therefore, the properties of the polymer can be fine-tuned to its respective requirement. In the current study, we investigated the influence of the isomer composition of the aforementioned diols on the thermal properties of polyesters.

In this context, we conducted an optimization of the hydroformylation reaction and developed modified synthesis strategies for diols **4** (Scheme 1). Our goal was to scale up the production process of compounds **3** and **4** to a multigram scale, aiming to produce amorphous polyesters with promising thermal properties. These polyesters show potential applications in food packaging and coil coating.

Results and discussion

Optimizing monomer synthesis for industrial-scale production

While the synthesis of diols from ENB (**1**) and VNB (**2**) has been previously described in a patent, the reported conditions required high temperatures and pressures, which are not ideal for large-scale production.[33] Furthermore, the available synthetic procedures and analytical data were limited. Given that diols **4** are excellent candidates for polyester monomers, the reaction sequence was re-evaluated to establish milder conditions that enhance scalability and reduce production cost.

ENB (**1**) and VNB (**2**) are commercially available as a mixture of *cis*/*trans* and/or *endo*/*exo* diastereomers, and the reactivity of their *endo*- and *exo*cyclic double bonds may influence the regioselectivity of their di-hydroformylation. Due to the inherent ring strain of the bicyclic structures, hydroformylation typically proceeds *via* an initial reaction at the *endo*cyclic double bond (**I**), followed by the less favoured hydroformylation of the *exo*cyclic double bond (**II**) (Scheme 2). Optimizing the reaction conditions, including pressure, temperature, reaction time, and phosphorus ligand selection, was therefore necessary to minimize undesired byproducts. The hydroformylation conditions were screened using bis(1,5-cyclooctadiene) rhodium(I) tetrafluoroborate $[Rh(COD_2)]BF_4$ as the precatalyst, in conjunction with the regio-directing phosphorus ligands Alkanox® and Oxophos®, which allow milder reaction conditions.[31,34,35] Additionally, (S_{ax},*S*,*S*)-bobphos[36,37] was tested, and a full screening of the reaction conditions did not improve conversion or regioselectivity. Consequently, due to these limitations and the scope of this study, this approach was not pursued further. For analysis, a combination of nuclear magnetic resonance (NMR) spectroscopy and gas chromatography mass spectrometry (GC MS) was employed due to the formation of multiple isomers, including diastereomers and regioisomers.

Hydroformylation experiments. The hydroformylation of ENB (**1**) was conducted with Alkanox® as the ligand at temperatures ranging from 40 to 140 °C in 20 °C increments, with an initial reaction time of three hours. The conversion was monitored by ^{1}H NMR spectroscopy. The characteristic resonances of the *endo*cyclic double bond were observed at δ_{1H} = 6.10 ppm and δ_{1H} = 6.05 ppm (**B**), while resonances at δ_{1H} = 5.42 ppm and δ_{1H} = 5.19 ppm (**C**) correspond to the *cis*/*trans* *exo*cyclic double bond (Fig. 1). At 40 and 60 °C, ENB (**1**) was

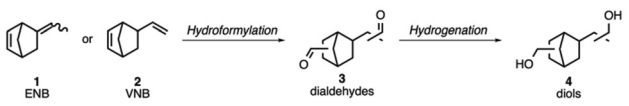

Scheme 1 Catalytic hydroformylation of ENB (**1**) or VNB (**2**) to a mixture of dialdehyde regioisomers (**3**) followed by hydrogenation to the corresponding diols (**4**).

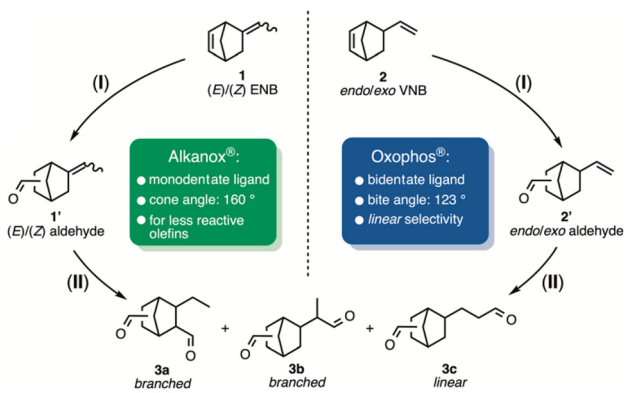

Scheme 2 Possible reaction sequences in di-hydroformylation of ENB (**1**) and VNB (**2**) using Alkanox® or Oxophos® as ligands.

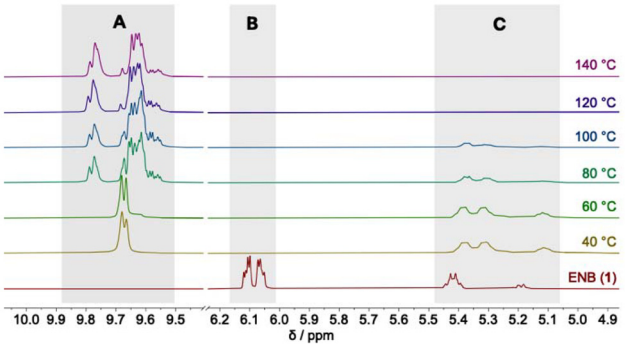

Fig. 1 Stacked ^{1}H NMR spectra from hydroformylation reactions of ENB (**1**) at different temperatures after three hours using Alkanox® as the ligand; reaction conditions: 0.10 mol% $[Rh(COD)_2]BF_4$, 0.35 mol% Alkanox®, CO/H_2 = 1/1, 50 bar, 40–140 °C, 3 h, (PhMe, 1 M). (A): characteristic resonances of aldehyde groups. (B): characteristic resonances of endocyclic double bonds. (C): characteristic resonances of *cis/trans* exocyclic double bonds.

fully converted to monoaldehydes **1′**, which subsequently formed dialdehydes **3** upon increasing the reaction temperature to 80 or 100 °C (**A**). The gradual shift in *exo*cyclic double bond resonances confirmed the formation of new products, with decreasing intensity at higher temperatures, indicating partial conversion of **1′** to dialdehydes **3** (**C**). At 120 and 140 °C, full conversion was achieved, and new aldehyde resonances between 9.0 and 10 ppm confirmed the presence of dialdehydes **3** (**A**).

The information gathered from the proton NMR spectra gave important insights into the reaction sequence of ENB (**1**) hydroformylation. However, signal overlap impeded further analysis and understanding of the reaction. Consequently, the experiments were also examined with GC MS and additional information could be collected (Fig. 2, left). Hydroformylation of ENB (**1**) at 40 and 60 °C resulted in aldehydes **1′** with exclusive mono-hydroformylation (m/z = 150). Increasing the temperature to 80 and 100 °C led to the desired dialdehydes **3** (m/z = 180), but with aldehydes **1′** being not yet fully converted. Full conversion of aldehydes **1′** was achieved at 120 and 140 °C, but partial reduction of the desired product was observed as a side reaction (m/z = 182). Thus, for initial scale-up, the reaction was performed overnight at 100 °C to achieve full conversion of **1′** without the formation of undesired by-products.

Despite the use of Alkanox® to control regioselectivity in ENB (**1**) hydroformylation, selectivity challenges remained. To address this, Oxophos® was used in the hydroformylation of VNB (**2**) to preferentially generate *linear* dialdehydes **3c**.[31] This approach leveraged VNB's (**2**) less sterically hindered *exo*cyclic double bond, in combination with the regio-directing effects of Oxophos®, facilitating the selective formation of *linear* dialdehydes **3c**. Examination of the reaction between 40 and 140 °C using a syngas ratio of CO/H_2 = 1/1 resulted in a mixture of products (Fig. 2, middle). Across this temperature range, byproducts **5a** (m/z = 122) and **5b** (m/z = 124) were detected along with aldehydes **2′** (m/z = 150) and **2″** (m/z = 152). Compared to the reaction of ENB (**1**) with Alkanox® (Fig. 2, left) the number of signals for dialdehydes **3** decreased and could be assigned to *linear* dialdehydes **3c** by ^{1}H and ^{13}C NMR spectroscopy. In an attempt to prevent reduction as a side reaction, the syngas ratio of CO/H_2 was adjusted from 1/1 to 3/2 (Fig. 2, right).[35,38] At 40 °C, aldehydes **2′** and byproduct **2″** were observed along with the desired *linear* dialdehydes **3c**, but the formation of **2′** and **2″** was significantly decreased at

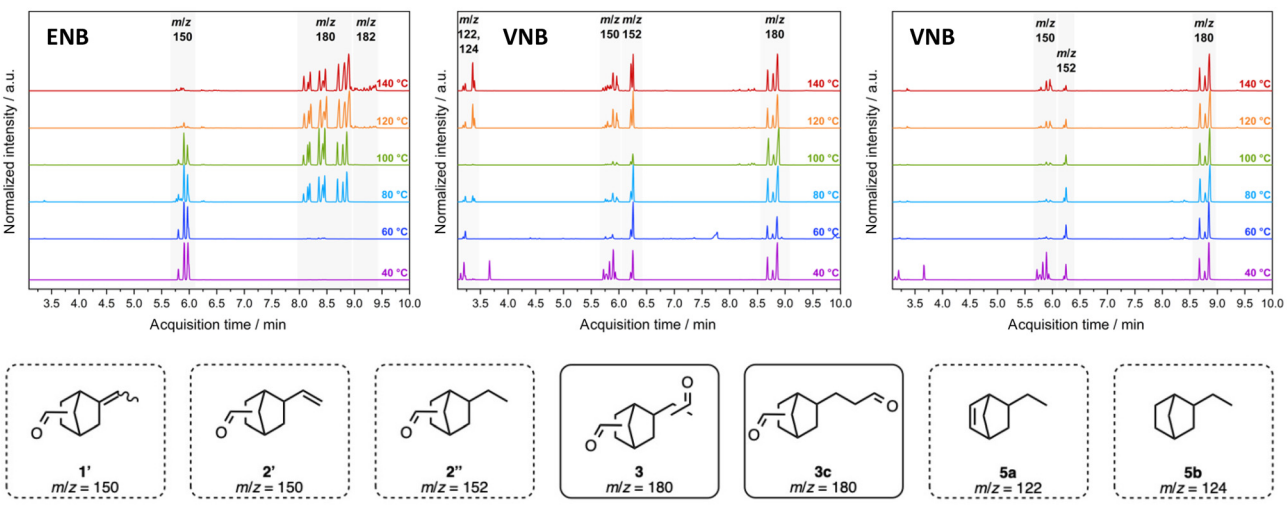

Fig. 2 Stacked GC chromatograms from hydroformylation reactions of ENB (**1**) and VNB (**2**) at different temperatures after three hours; reaction conditions: (left) 24.96 mmol ENB (**1**), 0.10 mol% $[Rh(COD)_2]BF_4$, 0.31 mol% Alkanox®, CO/H_2 = 1/1, 50 bar, 40–140 °C, (PhMe, 1 M). (middle) 24.96 mmol VNB (**2**), 0.10 mol% $[Rh(COD)_2]BF_4$, 0.11 mol% Oxophos®, CO/H_2 = 1/1, 50 bar, 40–140 °C, (PhMe, 1 M). (right) 24.96 mmol VNB (**2**), 0.10 mol% $[Rh(COD)_2]BF_4$, 0.11 mol% Oxophos®, CO/H_2 = 3/2, 50 bar, 40–140 °C, (PhMe, 1 M). Byproducts: aldehydes **1′** (m/z = 150) result from ENB (**1**) hydroformylation; aldehydes **2′** (m/z = 150) and **2″** (m/z = 152) result from VNB (**2**) hydroformylation; hydrogenated compounds **5a** (m/z = 122) and **5b** (m/z = 124) emerge as byproducts from VNB (**2**) hydroformylation with a syngas ratio of CO/H_2 = 1/1.

higher temperatures (60–100 °C). At 120 and 140 °C, the signal intensities of **2′** and **2″** increased again, presumably due to the decomposition of the ligand Oxophos®.[39] Therefore, the best result was obtained at 100 °C and CO/H_2 = 3/2, and these conditions were used for the initial scale-up.

To explore iso-selective hydroformylation of *branched* dialdehydes **3a** + **3b**, the chiral ligand (S_{ax},*S*,*S*)-bobphos was tested with ENB (**1**). Reactions were conducted at 40–80 °C (CO/H_2 = 1/1) for 24 h and analysed by GC MS. At 40 °C, mainly aldehydes **1′** were formed. At 60 °C, a mixture of *branched* dialdehydes **3a** + **3b** and aldehydes **1′** was detected. At 80 °C, selectivity decreased due to the formation of a mixture of **3** and undesired reduction products. Further screening of catalyst and ligand loading at 60 °C did not improve conversion or regioselectivity, and consequently, this approach was not pursued further.

The hydroformylation reactions were optimized for scalability by adjusting the temperature and pressure in Rh-catalysed reactions of ENB (**1**) and VNB (**2**). Initial scale-up was performed in a 2 L batch reactor with a batch size of 416 mmol. Purification *via* vacuum distillation yielded colourless liquids with 76% yield for dialdehydes **3** and 40% yield for *linear* dialdehydes **3c**. Despite high conversions, yield losses were observed during vacuum distillation, likely due to viscosity increases in the residue. Gradual temperature increases were applied to mitigate yield loss, but aldehyde side reactions (*e.g.* dehydrogenation or decomposition) may occur due to the low decomposition temperature of dialdehydes **3** (T_d = 107 °C, see the ESI†). Moreover, stability studies of dialdehydes **3** revealed acetalization as a potential side reaction, which was identified using FT-IR and ESI-MS (see ESI Fig. S2 and Table S1†).

Hydrogenation experiments. The hydrogenation of dialdehydes **3** and *linear* dialdehydes **3c** was investigated using two different approaches: (a) hydrogenation of the crude product mixture and (b) hydrogenation of the previously purified dialdehydes **3** and *linear* dialdehydes **3c**.[40]

Initial hydrogenation attempts of dialdehydes **3** were conducted following strategy (a) on a 24.96 mmol scale, using 2 wt% RANEY® nickel and 10 wt% H_2O. The addition of water could significantly improve the yield; thus, water was incorporated into the crude reaction mixture of **3** post-hydroformylation.[40] The reactions were evaluated across a temperature range of 25 to 140 °C at 50 bar H_2, and the desired products were subsequently isolated *via* vacuum distillation (Table 1). Reaction progress was meticulously monitored using GC MS (see ESI Fig. S1†). Alongside the formation of diols **4** (*m*/*z* = 184, **C3**; see ESI Fig. S1†), byproducts such as partially reduced compounds (*m*/*z* = 182; **C2**, Fig. S1†) and unreacted dialdehydes **3** were also detected (*m*/*z* = 180, **C1**; see ESI Fig. S1†). Additionally, light-boiling byproducts from the hydroformylation step remained in the reaction mixture (**A** and **B**; see ESI Fig. S1†). The desired products **4** were successfully isolated after full conversion of **3** with yields ranging from 45% to 67%, based on ENB (**1**), using vacuum distillation. For comparison, the patent procedure using dicyclopentadiene (DCPD) achieved a 71% yield of TCD-DM.[40] Prolonged reaction times

Table 1 Hydrogenation of a crude product mixture of dialdehydes **3** using RANEY® nickel as the catalyst in toluene/H_2O solution (o.n. = overnight: >16 h), n.d. = not determined when full conversion of **3** was not completed; reaction conditions: 24.96 mmol **3**, 2 wt% RANEY® nickel, 10 wt% H_2O, 50 bar H_2

#	*T* [°C]	H_2 usage [bar]	Time [h]	Yield [%]	Full conversion of **3**
1	r.t.	5.0	o.n.	n.d	No
2	40	6.0	o.n.	45	Yes
3	60	7.5	o.n.	n.d.	No
4	80	9.0	o.n.	66	Yes
5	100	10	o.n.	66	Yes
6	120	9.0	14	n.d.	No
7	140	10	4.5	67	Yes

exceeding 14 hours were noted at temperatures below 140 °C. However, at 140 °C, hydrogenation was completed within five hours. Trace amounts of the Rh-catalyst could interfere with conversion rates and hinder product isolation during vacuum distillation. Consequently, strategy (b) was employed for the reduction of purified dialdehydes **3**, leading to improved yields. The initial scale-up was conducted at a 171 mmol scale at 140 °C under optimized conditions using 4 wt% RANEY® nickel and 20 wt% H_2O, yielding 82% diols **4** (Scheme 3).

Simultaneously, the hydrogenation of *linear* dialdehydes **3c** was conducted on the crude product mixture at reaction temperatures of 80 °C and 100 °C. The resulting yields ranged from 16% to 31%, which are considerably lower compared to the hydrogenation of dialdehydes **3**. In both cases, the catalyst concentration was maintained at 2 wt% RANEY® nickel with 10 wt% H_2O. To achieve complete conversion of *linear* dialdehydes **3c** while preventing undesired side reactions, temperatures of at least 80 °C were deemed sufficient. Based on the previously optimized hydrogenation conditions of **3** using 4 wt% RANEY® nickel and 20 wt% H_2O, the hydrogenation process was successfully implemented on a 155 mmol scale. Hydrogenation of purified **3c** at 90 °C resulted in a 60% yield of *linear* diols **4c** (Scheme 3).

Proof-of-concept synthesis of *branched* diols 4b

The targeted synthesis of *linear* diols **4c** suggests the possibility of selectively synthesizing *branched* dialdehydes. This

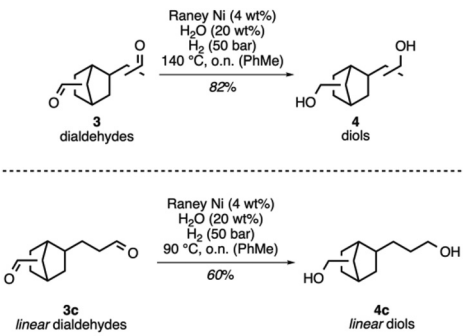

Scheme 3 Optimized hydrogenation strategy for the scale-up synthesis of diols **4** and *linear* diols **4c**.

approach may aid in screening structural dependencies on the thermal properties of polyesters. Building on the observed differences in the nature of the *endo*- and *exo*cyclic double bonds of ENB (**1**) and VNB (**2**) under hydroformylation conditions, an alternative route towards *branched* diols **4b** was investigated (Scheme 4).[41] Therefore, the *branched* moiety in **3b** was designed in two steps *via* the Wittig reaction, followed by hydrolysis. The substrate 5-acetyl-2-norbornene (AcNB, **6**) was converted with *in situ* generated phosphorus ylide (methoxymethylene)triphenyl phosphane to *cis*/*trans* enolether **7** in 92% yield. The hydrolysis was performed with 20 mol% *p*-toluenesulfonic acid monohydrate, affording the corresponding *branched* aldehyde **8** in 84% yield. These two transformations laid the foundation for the *branched* moiety in **4b**. Hence, the *endo*cyclic double bond in **8** was implemented with the Rh-catalysed hydroformylation using Alkanox® as the ligand. The crude product **3b** was initially reduced with $NaBH_4$ and MeOH to the corresponding *branched* diols **4b**. After purification with silica gel column chromatography, compound **4b** was isolated in 64% yield. The alternative route towards *branched* diols **4b** might not provide industrial scalability, but it allowed access to *branched* isomers. Hence, the three diols **4**, **4b**, and **4c** possess structural differences and could show an intriguing influence on the thermal properties in polyester synthesis.

Synthesis of amorphous polyesters and thermal structure–property relationships

To investigate the impact of *branched* and *linear* moieties on the polyester microstructure, diols **4**, **4b**, and **4c** were synthesized and incorporated into polyesters *via* a two-step melt polycondensation reaction using dimethyl terephthalate (DMT) as a model compound. Titanium tetra-*n*-butoxide [Ti(O*n*Bu)$_4$, 0.20 mol%] was employed as a catalyst (Scheme 5) to facilitate polymerization and enable a comparative study of the structural influence on material properties. DMT was selected for its well-characterized thermal properties, allowing direct comparison with commercially relevant poly(ethylene terephthalate)s. Additionally, this method accommodates bio-based diacids of diesters such as dimethyl furan dicarboxylate (DMFD).

While purified terephthalic acid (TPA) is the predominant monomer in PET production, its use in laboratory-scale synthesis poses challenges due to the presence of residual carboxylic acid groups, which can lead to side reactions, hinder chain growth, and potentially worsen alcoholysis. These issues

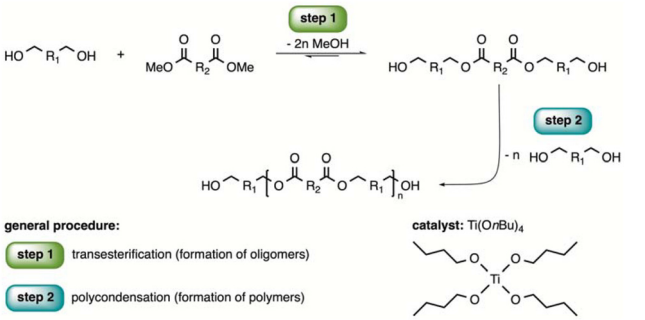

Scheme 5 General polycondensation procedure for polyester synthesis (R_1/R_2: alkyl).

are especially pronounced with thermally sensitive diols, such as 1,4-butanediol, which may undergo dehydration to tetrahydrofuran (THF) under esterification conditions.

In the transesterification step, a diol-to-diester mixture (2 : 1 molar ratio) was heated to 160 °C under ambient pressure, initiating methanol evolution. The temperature was incrementally increased by 10 °C to 220 °C until methanol evolution ceased (~5 to 6 hours), forming oligomeric precursor esters (step 1, Scheme 5). Subsequently, under reduced pressure (0.05 mbar), the oligomeric mixture was heated to 240 °C for 2–3 hours to remove volatilized diols *via* distillation (step 2, Scheme 5). The resulting amber-coloured polymer melt was dissolved in dichloromethane, precipitated, washed with cold methanol, and dried overnight at 70 °C under vacuum, yielding colourless to pale yellow polyesters (P**4**T, P**4b**T, and P**4c**T).

Polymerization with diols **4** produced medium-to-high-molecular weight polymers ($M_{n,rel}$ = 7.89–19.2 kg mol^{-1}) with moderate to broad dispersities ($Đ$ = 1.65–4.74) (P**4**T1–4; see ESI Table S2†). While reaction conditions such as temperature, catalyst loading, and time were kept constant, the observed differences in molecular weight and dispersity across the P**4**T1–4 series are attributed to variations in the reaction scale. Initial reactions were performed on a smaller scale to assess monomer reactivity, followed by larger-scale polymerizations to obtain sufficient material for characterization. These scale differences likely influenced mixing efficiency and substrate dispersion, affecting polymer chain growth. Consistently, diols **4b** generated similar molecular weight distributions ($M_{n,rel}$ = 9.39–23.8 kg mol^{-1}) but with narrower dispersities ($Đ$ = 2.10–2.70) (P**4b**T1–4; see ESI Table S2†). However, the highest molecular weights in the P**4**T and P**4b**T series were obtained

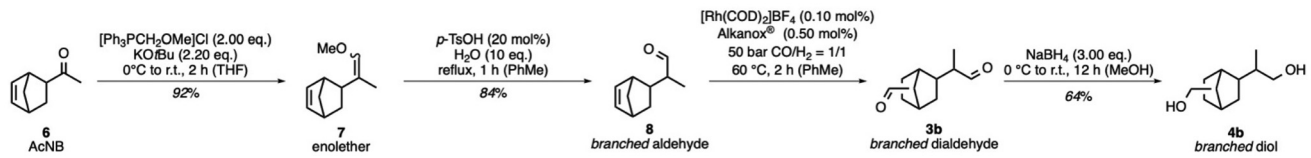

Scheme 4 Synthesis of *branched* dialdehydes **3b** *via* Rh-catalysed hydroformylation with Alkanox® as the ligand, followed by reduction to the corresponding *branched* diols **4b**.

with $M_{n,rel}$ = 19.2 kg mol^{-1} and $M_{n,rel}$ = 23.8 kg mol^{-1}. The polymer containing *linear* diols **4c** exhibited a high molecular weight ($M_{n,rel}$ = 12.8 kg mol^{-1}) with a broad dispersity ($Đ$ = 4.48) (Table 2).

Achieving high-molecular-weight polymers requires precise end-group stoichiometry and efficient condensate removal to drive the reaction equilibrium toward polymer formation. The observed constraints in molecular weights and broad dispersities are characteristic of polycondensation due to inherent challenges, including:

• The necessity for exact stoichiometric balance between diester and diol, as minor deviations significantly reduce achievable molecular weights.

• Potential alcohol elimination during heating, leading to unreactive chain ends. Gas chromatography (GC) analysis detected volatile alcoholysis byproducts from excess diols removed during polymerization.

For industrial scalability, solid-state polymerization (SSP) can enhance molecular weight; however, its applicability is typically limited to semicrystalline polymers and may therefore be restricted for the predominantly amorphous polyesters described in this work.[42–44]

Understanding the thermal behaviour of these polyesters is essential for evaluating their potential high-temperature applications. Thermogravimetric analysis (TGA) and differential scanning calorimetry (DSC) were used to assess decomposition temperatures (T_d) and glass transition temperatures (T_g), revealing strong correlations with polymer chain lengths and structural differences.

TGA revealed T_d values between 361 and 381 °C for the P**4**T series, while P**4b**T and P**4c**T demonstrated slightly higher T_d values up to 387 °C (see ESI Table S2†). While this trend reflects general increases in molecular weight, it also highlights the influence of chain uniformity. Notably, the P**4b**T series displayed narrower molecular weight distributions and more consistent TGA profiles than P**4**T, suggesting that structural uniformity contributes to thermal stability. The broader variability observed in P**4**T may stem from the mixed regioisomer content of diol **4**, which could lead to microstructural deviations or sequence blockiness, depending on differences in reactivity and volatility among the isomers. These factors warrant further investigations, particularly with purified diol isomers to assess their impact on polymer architecture and thermal behaviour.

DSC analysis further highlighted the relationship between molecular weight and T_g. The T_g of P**4**T increased progressively with molecular weight, reaching 100 °C at $M_{n,rel}$ = 19.2 kg mol^{-1}. The incorporation of *branched* moieties into P**4b**T resulted in higher T_g values reaching 103 °C at $M_{n,rel}$ = 23.8 kg mol^{-1}, whereas the incorporation of *linear* diols **4c** into P**4c**T notably reduced T_g to 75 °C at $M_{n,rel}$ = 12.8 kg mol^{-1}. The lower T_g of P**4c**T is consistent with its lower molecular weight and the presence of flexible *linear* alkyl side chains, both of which contribute to increased segmental mobility. Although the *linear* structure could facilitate tighter chain packaging, DSC analysis did not reveal any evidence of crystallinity (see ESI Fig. S28†). Compared to previously reported biobased polyesters, none were found to combine M_n above 20.0 kg mol^{-1} and T_g above 100 °C, highlighting the favourable thermal properties of P**4b**T.[12,20,28,45–51] Although direct comparison with commercial polyesters such as Tritan™ and PETG is premature due to differences in molecular weight and processing history, the reported T_g values (up to 103 °C) and thermal stability (T_d up to 387 °C) of the synthesized polyesters indicate promising potential for future development toward high-performance applications.

Incorporation of isosorbide into copolyesters: synthesis, characterization and thermal properties

The incorporation of isosorbide (IS, **9**; Fig. 3) as a renewable diol into polyesters has been widely studied due to its ability to significantly increase T_g while enhancing optical properties, including improved transmittance and reduced haze.[14] Additionally, dimethyl furan dicarboxylate (DMFD, **10**; Fig. 3) is emerging as a promising alternative to DMT in polyester production. Literature reports indicate that polyesters synthesized with DMFD exhibit thermal and barrier properties comparable to petroleum-based poly(ethylene terephthalate)s (PET), making them attractive for sustainable polymer development.[11,45,52,53]

In this study, a series of copolyesters – P**4***co*IST, P**4c***co*IST, and P**4***co*ISF – were synthesized using a well-established two-step melt polycondensation process. These copolyesters incorporated diols **4**, *linear* diols **4c**, and isosorbide (IS), with DMT (T) and DMFD (F) serving as the corresponding diesters. The

Table 2 Polycondensation of diols **4**, **4b** and **4c** with DMT (diol-to-diester ratio of 2 : 1) at 220–240 °C yielding the respective polyesters P**4**T, P**4b**T and P**4c**T

Polyester	$M_{n,rel}$ [a] [kg mol^{-1}]	$M_{w,rel}$ [a] [kg mol^{-1}]	$Đ$ [a] [—]	T_d [b] [°C]	T_g [c] [°C]
P**4**T	19.2	60.8	3.17	364	100
P**4b**T	23.8	63.3	2.70	379	103
P**4c**T	12.8	57.3	4.48	371	75

[a] Relative molecular weight and dispersity measured using GPC in THF at 30 °C (25 mmol L^{-1}) relative to polystyrene. [b] Onset decomposition temperatures (T_d) of the first decomposition step determined *via* TGA measurements. [c] T_g determined *via* DSC measurements.

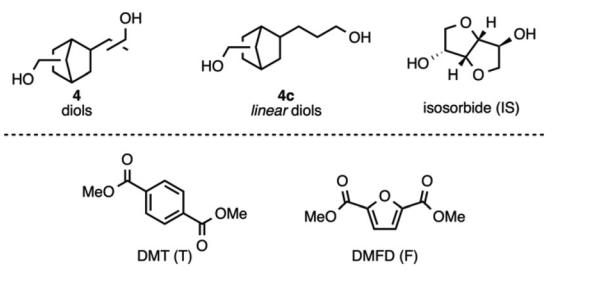

Fig. 3 Depicted diol and diester monomers for the synthesis of copolyesters P4*co*IST, P4c*co*IST and P4*co*ISF.

reaction was conducted using a diol-to-diacid molar ratio of 2 : 1. The chemical structures of the resulting copolyesters were characterized using ^{1}H NMR and DOSY NMR spectroscopy, while their thermal properties were evaluated using TGA and DSC. These properties were then compared to those of reference polyesters P4T and P4**c**T. Although diol **4b** demonstrated superior molecular control over molecular weight and dispersity, along with high T_g values, it was not included in the copolymerization due to the increased synthetic effort required for its preparation. The more scalable synthesis of diols **4** and **4c** made them more suitable for evaluating industrially relevant systems.

The incorporation of IS into copolyesters P4*co*IST, P4**c***co*IST, and P4*co*ISF presented specific challenges. Among these, P4*co*IST exhibited the lowest molecular weight with a narrow dispersity (Table 3). The ^{1}H NMR analysis confirmed the presence of characteristic resonances for DMT and ester groups (–CH_2O–) of diols **4** and **4c**, similar to those observed in polyesters P4T and P4**c**T. The aliphatic proton resonances of IS were identified between δ_{1H} = 5.51 and 4.00 ppm, with chain end groups appearing at δ_{1H} = 5.00 and 3.60 ppm. Aliphatic protons of DMFD were detected at δ_{1H} = 4.20 ppm and δ_{1H} = 1.10 ppm, respectively. By comparing the intensity peaks of aromatic protons in DMT and DMFD to those of the ester groups (–CH_2O–) of diols **4** and **4c**, the final molar ratios of IS in the copolyesters were determined (Table 3). DOSY NMR spectroscopy further confirmed successful copolymerization, as the diffusion coefficients of proton signals from DMT and DMFD were identical to those of the respective diols (see ESI Fig. S14, S16 and S18†).

Achieving high transesterification conversion, which facilitates polycondensation, requires efficient removal of alcohol byproducts to drive the reaction equilibrium. However, IS negatively impacted the polycondensation process, reducing the conversion rate and yielding shorter oligomers. Additionally, co-diols with lower boiling points than isosorbide reacted more quickly and evaporated more readily, further complicating the reaction.[14,54]

Despite these challenges, the transesterification step remained unaffected, with methanol evolution completing within 5–6 hours. However, the polycondensation step was more complex, relying on rapid alcoholysis and efficient elimination of terminal diols under high vacuum (<1 mbar). The boiling points of IS[14] and diols **4** overlapped (105–120 °C *vs.* 120 °C, respectively), complicating selective removal. *Linear* diols **4c** exhibited a slightly higher boiling point (130 °C), which influenced their behaviour in polycondensation. Our findings align with previous studies by Fenouillot *et al.*, who investigated the reactivity of IS. They found that primary bicyclic diols, such as diols **4** and **4c**, can induce steric hindrance, whereas the secondary bicyclic structure of IS allows for better accessibility to ester groups.[14] Furthermore, the hydrophobic properties of diols **4** and **4c** contrast with the hydrophilic properties of IS, making hydrophilic ester bond formation more challenging when diols **4b** or **4c** are present at both chain ends.[14] Fenouillot's study also suggested that IS can act as a promoter, accelerating the polycondensation step.[14]

Comparing the molecular weights of P4*co*IST ($M_{n,rel}$ = 7.37 kg mol^{-1}) and P4**c***co*IST ($M_{n,rel}$ = 17.3 kg mol^{-1}), it was evident that copolymerization of IS with *linear* diols **4c** resulted in higher molecular weights. This suggests that IS acted more effectively as a "chain linker" than *linear* diols **4c**, leading to a lower IS content (1.50 mol%) in P4**c***co*IST. In contrast, the copolymerization of IS with diols **4** proved more complex, likely due to a mixture of sterically hindered isomers (*branched vs. linear*). The overlapping boiling points further complicated the removal process, leading to a higher IS content in P4*co*IST (5.00 mol%) compared to P4**c***co*IST (1.50 mol%). These observations suggest that future studies should explore separating regioisomers **4a**, **4b**, and **4c** as model compounds to better understand reactivity differences between hydrophobic diols and hydrophilic IS.

Despite precipitation and methanol washing, P4*co*ISF (2.50 mol% IS content) exhibited a pale-yellow colour, a common issue associated with high polymerization temperatures.[11,45,53] Although DMFD was used to mitigate decarboxylation, prolonged reaction times (>16 hours) and high melt viscosity hindered heat and mass transfer. However, replacing DMT with DMFD provides significant advantages, including improved crystallization behaviour, ensuring amorphous morphologies suitable for industrial processing. Additionally, poly(ethylene 2,5-furanedicarboxylate) polyesters exhibit significantly lower gas permeabilities (O_2, CO_2, and H_2O) due to reduced chain mobility, making them promising candidates for food packaging applications.[11]

Thermal analysis using TGA and DSC revealed distinct structure–property relationships in copolyesters incorporating IS (Table 3). P4*co*IST and P4**c***co*IST demonstrated high thermal

Table 3 Polycondensation of diols **4**, **4b** and **4c** with IS and DMT/DMFD (diol-to-diester ratio of 2 : 1) at 220–240 °C yielding the respective copolyesters P4coIST, P4**c**coIST and P4coISF

Copolyester	Mole fraction of IS in the copolyester[a] [mol%]	$M_{n,rel}$[b] [kg mol^{-1}]	$M_{w,rel}$[b] [kg mol^{-1}]	$Đ$[b] [—]	T_d[c] [°C]	T_g[d] [°C]
P4*co*IST	5.00	7.4	12.9	1.76	373	97
P4**c***co*IST	1.50	17.3	38.5	2.07	363	81
P4*co*ISF	2.50	13.4	31.9	1.88	340	89

[a] Mole fraction of IS in the copolyester, determined by integration in ^{1}H NMR spectra. [b] Relative molecular weight and dispersity measured using GPC in THF at 30 °C (25 mmol L^{-1}) relative to polystyrene. [c] Onset decomposition temperatures (T_d) of the first decomposition step determined *via* TGA measurements. [d] T_g determined *via* DSC measurements.

stability, with T_ds of 373 °C and 363 °C, comparable to T_d = 363–379 °C (see ESI Table S2†) observed in reference polyesters P**4**T and P**4c**T. In contrast, P**4***co*ISF exhibited a lower T_d of 340 °C. Despite this, all copolyesters displayed excellent thermal stability, making them suitable for high-temperature applications such as injection molding. DSC analysis highlighted the influence of molecular weight on T_g. The T_g of P**4***co*IST (97 °C) was significantly higher than that of P**4**T1 (87 °C; see ESI Table S2†) despite similar molecular weights, aligning with previous studies that 6 mol% IS can increase T_g by 10 °C.[18] Conversely, the incorporation of 2.50 mol% IS into P**4***co*ISF did not significantly affect T_g, which remained at 89 °C, compared to 92 °C for the polyester P**4**T2 (see ESI Table S2†). In contrast, in the copolyester P**4c***co*IST, 1.50 mol% IS content increased T_g to 81 °C, compared to 75 °C in P**4c**T. This suggests that even a low IS content can have a noticeable influence on the thermal properties, particularly in systems incorporating *linear* diols. Additionally, the variation in T_g between different copolyesters highlights the importance of precise monomer selection and polymerization conditions to achieve desired thermal characteristics.

Further investigation into the molecular dynamics of these copolyesters could provide deeper insights into the structural effects of IS incorporation. Future studies could explore the interplay between chain rigidity, segmental mobility, and hydrogen bonding interactions to fully understand the role of rigid cyclic diols in polyester performance. Moreover, optimizing reaction conditions to further increase molecular weight while maintaining favourable thermal properties will be crucial for advancing these materials in industrial applications such as sustainable packaging and coatings.

Conclusions

This study highlights the potential of utilizing alicyclic-diene-based polyols as key components for synthesizing amorphous, high T_g polyesters. The successful synthesis and scale-up of dialdehydes **3** and **3c** were achieved through optimized hydroformylation reactions using two regio-directing ligands. The subsequent hydrogenation process to produce diols **4** and *linear* diols **4c** was effectively carried out using RANEY® nickel, a widely used industrial heterogeneous catalyst. Despite these advancements, further improvements in purification methods are necessary to maximize the yields of reactive dialdehydes.

Additionally, an alternative pathway for synthesizing *branched* diols **4b** was established, allowing for an investigation into the influence of different regio- and diastereomers on polyester properties. The synthesized diols **4**, **4b** and **4c** provided a platform for developing amorphous polyesters with medium-to-high molecular weights. While complete molecular weight optimization was not achieved, the resulting polyesters exhibit promising thermal properties, with T_g values ≥100 °C.

Although the synthesis of monomers **4** and **4c** still relies on petroleum-based raw materials, this work advances the development of partially biobased polyesters by incorporating sustainable building blocks such as IS and DMFD. Notably, the incorporation of 5.00 mol% IS into the P**4***co*IST-type copolyester significantly increased the glass transition temperature (T_g = 97 °C), despite its low molecular weight ($M_{n,rel}$ = 7.37 kg mol^{-1}). Similarly, in the P**4c***co*IST-type copolyester, IS incorporation increased T_g from 75 °C to 81 °C. The replacement of DMT with DMFD presents additional advantages in terms of mechanical and barrier properties. Although the P**4**coISF copolyester exhibited promising thermal properties, achieving higher molecular weight (M_n > 20 kg mol^{-1}) will be essential for optimizing mechanical performance.

Cycloaliphatic structures offer significant advantages not only in polyesters but also in poly(amide)s (PA),[54] poly(urethane)s (PU)[55] or poly(methyl methacrylate)s (PMMA).[56] Incorporating cycloaliphatic moieties into these polymers enhances their properties, making them more suitable for demanding applications that require enhanced UV stability, mechanical strength, and thermal resistance. These enhanced properties enable their use in a wide range of applications, including automotive parts, optical components, coatings, adhesives, and consumer goods.

The polymer precursors developed in this study open new avenues for synthesizing novel monomers, including amines, carboxylic acids, and methyl methacrylates. These advancements will facilitate the development of innovative copolymers tailored to meet the stringent requirements of high-performance applications, extending both the usability and lifespan of advanced materials.

Author contributions

Brigita Bratić: conceptualization, synthesis, funding acquisition, writing – original draft, visualization, data curation, and formal analysis; Peter Altenbuchner: writing – review & editing, visualization, data curation, and formal analysis; Thomas Heuser: writing – review & editing, visualization, data curation, and formal analysis; Bernhard Rieger: funding acquisition, supervision, project administration, resources, and writing – review & editing.

Data availability

The data supporting this article have been included as part of the ESI.†

Conflicts of interest

There are no conflicts to declare.

Acknowledgements

The authors want to thank Dr Fabian Martin Hörmann and Stefanie Hörl for the great proofreading process. Additionally,

the authors are grateful for the good discussion with the group of the WACKER Chair of Macromolecular Chemistry and Evonik Industries. The authors additionally want to thank Evonik Industries for support and funding.

References

1 R. Hatti-Kaul, L. J. Nilsson, B. Zhang, N. Rehnberg and S. Lundmark, *Trends Biotechnol.*, 2019, **38**, 1–67.
2 R. Mori, *RSC Sustainability*, 2023, **1**, 179–212.
3 M. Zhang, G. M. Biesold, W. Choi, J. Yu, Y. Deng, C. Silvestre and Z. Lin, *Mater. Today*, 2022, **53**, 134–161.
4 V. T. Weligama Thuppahige and M. A. Karim, *Compr. Rev. Food Sci. Food Saf.*, 2022, **21**, 689–718.
5 C. Lambré, J. M. Barat Baviera, C. Bolognesi, A. Chesson, P. S. Cocconcelli, R. Crebelli, D. M. Gott, K. Grob, E. Lampi, M. Mengelers, A. Mortensen, G. Rivière, V. Silano, I. L. Steffensen, C. Tlustos, L. Vernis, H. Zorn, M. Batke, M. Bignami, E. Corsini, R. Fitzgerald, U. Gundert-Remy, T. Halldorsson, A. Hart, E. Ntzani, E. Scanziani, H. Schroeder, B. Ulbrich, D. Waalkens-Berendsen, D. Woelfle, Z. Al Harraq, K. Baert, M. Carfì, A. F. Castoldi, C. Croera and H. Van Loveren, *EFSA J.*, 2023, **21**, e06857.
6 J. S. Siracusa, L. Yin, E. Measel, S. Liang and X. Yu, *Reprod. Toxicol.*, 2018, **79**, 96–123.
7 A. Abraham and P. Chakraborty, *Rev. Environ. Health*, 2019, **2**, 201–210.
8 Y. B. Wetherill, B. T. Akingbemi, J. Kanno, J. A. McLachlan, A. Nadal, C. Sonnenschein, C. S. Watson, R. T. Zoeller and S. M. Belcher, *Reprod. Toxicol.*, 2007, **24**, 178–198.
9 S. Mangaraj, A. Yadav, L. M. Bal, S. K. Dash and N. K. Mahanti, *J. Package Technol. Res.*, 2019, **3**, 77–96.
10 F. Fenouillot, A. Rousseau, G. Colomines, R. Saint-Loup and J.-P. Pascault, *Prog. Polym. Sci.*, 2010, **35**, 578–622.
11 D. Zhang and M. J. Dumont, *J. Polym. Sci., Part A: Polym. Chem.*, 2017, **55**, 1478–1492.
12 J. Wang, X. Liu, Z. Jia, Y. Liu, L. Sun and J. Zhu, *J. Polym. Sci., Part A: Polym. Chem.*, 2017, **55**, 3298–3307.
13 M. N. S. Kumar, Z. Yaakob and H. Siddaramaiah, in *Handbook of Bioplastics and Biocomposites Engineering Applications*, ed. S. Pilla, 2011, pp. 121–160.
14 S. Legrand, N. Jacquel, H. Amedro, R. Saint-Loup, M. Colella, J.-P. Pascault, F. Fenouillot and A. Rousseau, *ACS Sustainable Chem. Eng.*, 2020, **8**, 15199–15208.
15 J. Thiem and H. Lüders, *Polym. Bull.*, 1984, **11**, 365–369.
16 R. Storbeck, M. Rehahn and M. Ballauff, *Makromol. Chem.*, 1993, **194**, 53–64.
17 R. Storbeck and M. Ballauff, *J. Appl. Polym. Sci.*, 1996, **59**, 1199–1202.
18 H. R. Kricheldorf, G. Behnken and M. Sell, *J. Macromol. Sci., Part A: Pure Appl. Chem.*, 2007, **44**, 679–684.
19 R. Storbeck and M. Ballauff, *Polymer*, 1993, **34**, 5003–5006.
20 W. J. Yoon, S. Y. Hwang, J. M. Koo, Y. J. Lee, S. U. Lee and S. S. Im, *Macromolecules*, 2013, **46**, 7219–7231.
21 T. Kim, J. M. Koo, M. H. Ryu, H. Jeon, S.-M. Kim, S.-A. Park, D. X. Oh, J. Park and S. Y. Hwang, *Polymer*, 2017, **132**, 122–132.
22 S. Legrand, N. Jacquel, H. Amedro, R. Saint-Loup, J.-P. Pascault, A. Rousseau and F. Fenouillot, *Eur. Polym. J.*, 2019, **115**, 22–29.
23 S. R. Turner, *J. Polym. Sci., Part A: Polym. Chem.*, 2004, **42**, 5847–5852.
24 R. Quintana, A. M. De Ilarduya, A. Alla and S. Muñoz-Guerra, *J. Polym. Sci., Part A: Polym. Chem.*, 2011, **49**, 2252–2260.
25 G. W. Baell, C. E. Powell, J. Hancock, M. Kindinger, H. R. McKenzie, A. V. Bray and C. J. Booth, *Appl. Clay Sci*, 2007, **37**, 295–306.
26 M. Zhang, R. B. Moore and T. E. Long, *J. Polym. Sci., Part A: Polym. Chem.*, 2012, **50**, 3710–3718.
27 J. Wang, S. Mahmud, X. Zhang, J. Zhu, Z. Shen and X. Liu, *ACS Sustainable Chem. Eng.*, 2019, **7**, 6401–6411.
28 J. Wang, X. Q. Liu, Y. J. Zhang, F. Liu and J. Zhu, *Polymer*, 2016, **103**, 1–8.
29 S. Hong, K.-D. Min, B.-U. Nam and O. O. Park, *Green Chem.*, 2016, **18**, 5142–5150.
30 J. Wang, X. Q. Liu, Z. Jia, L. Sun, Y. J. Zhang and J. Zhu, *Polymer*, 2018, **137**, 173–185.
31 R. Franke, D. Selent and A. Börner, *Chem. Rev.*, 2012, **112**, 5675–5732.
32 Y. G. Osokin, *Pet. Chem.*, 2007, **47**, 1–11.
33 D. Mijolovic, V. Wendel and A. Suckert, BASF SE, *WO Pat.*, WO2011023540A2, 2011.
34 A. Bara-Estaún, C. L. Lyall, J. P. Lowe, P. G. Pringle, P. C. J. Kamer, R. Franke and U. Hintermair, *Faraday Discuss.*, 2021, **229**, 422–442.
35 C. Kubis, R. Ludwig, M. Sawall, K. Neymeyr, A. Börner, K.-D. Wiese, D. Hess, R. Franke and D. Selent, *ChemCatChem*, 2010, **2**, 287–295.
36 G. M. Noonan, J. A. Fuentes, C. J. Cobley and M. L. Clarke, *Angew. Chem.*, 2012, **124**, 2527–2530.
37 P. Dingwall, J. A. Fuentes, L. E. Crawford, A. M. Z. Slawin, M. Bühl and M. L. Clarke, *J. Am. Chem. Soc.*, 2017, **139**, 15921–15932.
38 D. Selent, R. Franke, C. Kubis, A. Spannenberg, W. Baumann, B. Kreidler and A. Börner, *Organometallics*, 2011, **30**, 4509–4514.
39 B. Kreidler, D. Fridag, B. Schemmer, B. Wechsler, A. Christiansen and D. Neumann, Evonik Oxeno GmbH, *EP Pat.*, EP2663573B2, 2011.
40 W. Dukat, E. Storm and K. Schmid, Oxea Deutschland GmbH, *US Pat.*, US7301057B2, 2005.
41 P. A. Byrne and D. G. Gilheany, *Chem. Soc. Rev.*, 2013, **42**, 6670–6696.
42 S. N. Vouyiouka, E. K. Karakatsani and C. D. Papaspyrides, *Prog. Polym. Sci.*, 2005, **30**, 10–37.
43 F. C. Chen, R. G. Griskey and G. H. Beyer, *AIChE J.*, 1969, **15**, 680–685.
44 K. D. Samant and K. M. Ng, *AIChE J.*, 1999, **45**, 1808–1829.
45 R. J. I. Knoop, W. Vogelzang, J. Van Haveren and D. S. Van Es, *J. Polym. Sci., Part A: Polym. Chem.*, 2013, **51**, 4191–4199.

46 J. G. Wang, X. Q. Liu, J. Zhu and Y. Jiang, *Polymers*, 2017, **9**, 305.
47 J. G. Van Berkel, N. Guigo, J. J. Kolstad, L. Sipos, B. Wang, M. A. Dam and N. Sbirrazzuoli, *Macromol. Mater. Eng.*, 2015, **300**, 466–474.
48 M. Jiang, Q. Liu, Q. Zhang, C. Ye and G. Zhou, *J. Polym. Sci., Part A: Polym. Chem.*, 2012, **50**, 1026–1036.
49 M. Vannini, P. Marchese, A. Celli and C. Lorenzetti, *Green Chem.*, 2015, **17**, 4162–4166.
50 G. Z. Papageorgiou, D. G. Papageorgiou, Z. Terzopoulou and D. N. Bikiaris, *Eur. Polym. J.*, 2016, **83**, 202–229.
51 M. Garaleh, T. Yashiro, H. R. Kricheldorf, P. Simon and S. Chatti, *Macromol. Chem. Phys.*, 2010, **211**, 1206–1214.
52 J. C. Morales-Huerta, A. Martínez de Ilarduya and S. Muñoz-Guerra, *Polymer*, 2016, **87**, 148–158.
53 W. H. Carothers, *Trans. Faraday Soc.*, 1936, **32**, 39–49.
54 C.-W. Chen, C.-W. Lin, Y.-H. Chen, T.-F. Wei, S.-P. Rwei and R. Sasikumar, *Polym. Bull.*, 2020, **77**, 235–253.
55 A. Mouren and L. Avérous, *Chem. Soc. Rev.*, 2023, **52**, 277–317.
56 S. K. Asha, V. Deepthimol and M. Lekshmi, *J. Polym. Sci., Part A: Polym. Chem.*, 2004, **42**, 5617–5626.